arXiv:cond-mat/9709085v1 [cond-mat.supr-con] 6 Sep 1997

Systematics of two-component superconductivity in $YBa_2Cu_3O_{6.95}$ from microwave measurements of high quality single crystals

H.Srikanth, Z.Zhai and S.Sridhar
Department of Physics, Northeastern University, 360 Huntington Avenue,
Boston, MA 02115

A. Erb and E. Walker
DPMC, Universite de Geneve, Geneve, Switzerland

(February 1, 2008)

A systematic set of microwave measurements of the surface impedance ($Z_s = R_s + iX_s$) of $YBa_2Cu_3O_{6.95}$ single crystals (called $YBCO/BZO$) grown in $BaZrO_3$ crucibles reveal new properties that are not directly seen in similar measurements on other $YBCO$ samples. The complex conductivity $\sigma = \sigma_1 - i\sigma_2$ obtained as a function of temperature (T) from the surface impedance data shows two key features : (1) A new conductivity peak in $\sigma_1(T)$ around $80K$ in addition to peaks at $30K$ and $92K$, and, (2) extra pairing below $65K$ in addition to the onset of pairing below the bulk T_c of $93.4K$ as revealed in $\sigma_2(T)$. These features are present in all 3 $YBCO/BZO$ crystals measured and are absent in $YBCO$ crystals grown by other methods. These results show that in addition to pairing at $T_c = 93.4K$, an additional pairing channel opens up at ($\sim 65K$).

High pressure oxygenation of one of the crystals still yields the same results, and shows that the data cannot be due to unwanted macroscopic segregation of O -deficient regions. Systematics on three single crystals show that the height of the quasiparticle conductivity peak at $80K$ in the superconducting state is correlated with the inelastic scattering rate in the normal state. Close to T_c, $\sigma_2(T) \sim (T_c - T)$, indicating a mean-field behavior and inconsistent with $3DXY$ fluctuations.

A single complex order parameter cannot describe these data, and the results suggest that at least two superconducting components with corresponding pairing temperature scales ($T_A \sim 65K$ and $T_B = T_c = 93.4K$) are required. Comparison to model calculations considering various decoupled two-component scenarios ($A + B = d + s, s + d, d + d$) are presented. The comparison shows that the experimental data do not distinguish between these various scenarios, however the data do require that one of the components be an order parameter (OP) with nodes in the gap, such as a $d-$ wave OP. Fit parameters to the calculations using the different scenarios are presented. These components are naturally present in all $YBCO$ samples, however impurities appear to suppress the pair density of the low temperature A component and lead to greatly enhanced scattering of the high temperature B component. Overall, our results strongly suggest the presence of multiple pairing temperature scales and energies in $YBa_2Cu_3O_{6.95}$.

I. INTRODUCTION

The order parameter of high temperature superconductors has been extensively studied recently, and a consensus seems to have emerged in favor of a d-wave order parameter (OP) [1]. However there are some notable indications (see ref. [2,3] for a summary) which suggest that, particularly in the most widely studied material, $YBa_2Cu_3O_{6.95}$, a pure d-wave OP may not occur and that there are indications of a multi-component OP (*eg.* s + d).

Material purity is crucial for studies of fundamental physical properties not obscured by impurity-related artifacts. This fact has been validated time and again in experiments on oxide superconductors as well as other materials. It is now accepted that improvement in material quality has often resulted in a better understanding of the physical properties in solid state systems.

The recent growth of $YBa_2Cu_3O_{7-\delta}$ single crystals in $BaZrO_3(BZO)$ crucibles has ushered in a new generation of ultra-pure samples [4]. This growth method avoids the critical problem of crucible corrosion and leads to single crystals with extremely clean surfaces and purity exceeding 99.995%. In contrast, the best crystals grown in conventional crucibles like Au and yttria-stabilized-zirconia (YSZ) have final reported purities of $99.5 - 99.95\%$ [5,6] A number of experiments on $YBCO/BZO$ crystals have revealed new features which are either greatly suppressed or not present in $YBCO/YSZ$ samples. We have recently observed novel features in the microwave surface impedance of $YBCO/BZO$ which clearly indicates the presence of two superconducting components [7].

In this paper, we present further evidence on the systematics in three $YBCO/BZO$ crystals. The results obtained confirm our earlier findings [7], *viz.* : (1) A new conductivity peak in $\sigma_1(T)$ around 80K which is correlated with the normal state scattering rate and (2) Extra pairing below 65K in addition to onset of pairing below the bulk T_c of $93.4K$ as revealed in $\sigma_2(T)$. *A single complex order parameter cannot describe these data and the data indicate the presence of at least two pairing pro-*

cesses, leading to at least two OP components. Model calculations considering various simple two-component scenarios (decoupled $d+s$ and $d+d$) and are presented. We show that the two-component picture can provide a quantitative description of the data, whereas a single order parameter (of any symmetry) does not. In addition the two-component picture can provide a description of the data on the earlier generation of $YBCO/YSZ$ crystals also. Analysis of the data close to T_c is not consistent with $3DXY$ fluctuations and displays a mean-field behavior. Systematics on three single crystals show a correlation between the inelastic scattering rate in the normal state with the quasiparticle conductivity peak at 80K in the superconducting state. We show that while a T-dependent scattering rate is required to quantitatively describe the conductivity peaks, the two-component scenario provides a natural explanation for the location of the $30K$ and $80K$ peaks in $\sigma_1(T)$ as arising from pairing at $65K$ and $93K$ respectively, in contrast with earlier interpretation of $YBCO/YSZ$ data which associated the $30K$ peak with pairing at $93K$. Overall, our results show that *a pure $d-wave$ state does not occur in $YBa_2Cu_3O_{6.95}$* and strongly suggest the presence of multiple pairing energies in $YBa_2Cu_3O_{6}.95$.We note that several microscopic pairing scenarios are consistent with the conclusions of this paper.

A. Properties of $YBCO/BZO$ crystals

One of the causes for the presence of impurities in $YBa_2Cu_3O_{7-\delta}$ single crystals is the random substitution at the Cu chain sites by trace amounts of crucible constituents like Au during the melt growth process. This results in local variation of oxygen vacancy distribution, introduction of magnetic moments and other local defects [8–10]. Although the overall T_c and sharpness of the superconducting transition may not be affected by a combination of these elements associated with impurities, important features of the superconducting ground state like the order parameter symmetry, scattering, superfluid density etc. are likely to be influenced. It is precisely these local impurities which are eliminated in (BZO) grown $YBa_2Cu_3O_{7-\delta}(YBCO)$ crystals thus providing an opportunity to probe the intrinsic ground state properties free from defects. Elimination of the metallic impurities also leaves oxygen stoichiometry as the only variable which needs to be controlled [8].

It is important to emphasize at this juncture that several new results have been obtained on these new generation crystals by a number of experimenters using a variety of probes like thermal, magnetic and electrodynamic response, and have led to a clearer picture of the nature of superconductivity in $YBa_2Cu_3O_{6.95}$. These results are :

(1) Clear imaging of the flux lattice of $YBCO$ using low temperature STM [11]. Thus far this has only been feasible with the new $YBCO/BZO$ crystals.

(2) “Fishtail effect” in magnetization *eliminated* in high pressure oxygen annealed $YBCO_{7.0}/BZO$ and optimally doped $YBCO/BZO$ samples [12].

(3) Schottky contribution to specific heat *suppressed* in $YBCO_{7.0}/BZO$ indicating the total absence of magnetic moments [13,14].

(4) The microwave conductivities $\sigma_1(T)$ and $\sigma_2(T)$ exhibit *two* distinct features not consistent with a single superconducting order parameter [7].

(5) The vortex lattice imaged with STM shows two different regions which is either representative of two superconducting components or two types of ordered oxygen clusters [15].

(6) Clear observation of a direct first order melting transition in $YBCO_{7.0}/BZO$ from a vortex lattice to liquid without an intervening glassy state [16].

(7) Evidence of extremely low J_c in $YBCO_{7.0}/BZO$ crystals indicative of very low pinning.

In an attempt to bring forth the essential differences, we have presented a comparison of some material and physical properties of $YBCO/YSZ$ and $YBCO/BZO$ crystals in a tabular form in Table I.

II. EXPERIMENTAL RESULTS

The microwave measurements were carried out in a $10GHz$ Nb cavity using a “hot finger” technique [17]. We measure the surface impedance $Z_s = R_s + iX_s$ and penetration depth $\lambda(= X_s/\mu_0\omega)$ as functions of temperature T, from which we extract the complex conductivity $\sigma_s = \sigma_1 - i\sigma_2$. This method has been extensively validated by a variety of measurements on cuprates and borocarbide superconductors [18,19].

Three single crystals (labeled AE103, AE105 and AE180 and typically $1.3 \times 1.3 \times 0.1mm^3$ in size) from different batches grown in BZO crucible and one crystal (labeled AEXX) of comparable dimensions grown in YSZ crucible were measured to study the systematics in the different samples. While standard oxygen annealing procedures at atmospheric pressure were followed to obtain optimally doped crystals with oxygen stoichiometry around $O_{6.95}$ in AE103, AE105 and AEXX, the AE180 sample was annealed at a pressure of 100 *bars* for 20 hours. Note that this high pressure annealing results in elimination of the formation of oxygen vacancy clusters and as a consequence, the “fishtail” anomaly in magnetization is suppressed. The crystals (AE103, AE105 and AE180) grown in BZO had $T_c = 93.4K$ and AEXX had $T_c = 92.4K$. All four crystals exhibited very narrow transitions in $R_s(T)$ at 10 GHz of $< 0.3K$.

The temperature dependence of surface resistance $R_s(T)$ and change in penetration depth $\Delta\lambda(T)$ were presented for AE103 and AEXX crystals and discussed in detail in an earlier publication [7]. In this paper, we show that the data for AE105 and AE180 crystals also show the new features seen in the AE103 single crystal. The data for all the three high purity $YBCO/BZO$ crystals clearly reveal a new bump in the vicinity of $60K$ which is not seen in $YBCO/YSZ$. Also the estimated London penetration depth $\lambda(0)$ for $YBCO/BZO$ samples are $\simeq 1000\mathring{A}$ which is lower than the value of $1400\mathring{A}$ estimated for the $YBCO/YSZ$ crystal. We obtain the absolute value of X_s by equating $R_n = X_n$ above T_c.

Since the absolute values of $R_s(T)$ and $X_s(T)$ are now known, we can plot the amplitude $\mid Z_s(T) \mid \equiv \sqrt{R_s(T)^2 + X_s(T)^2}$ as a function of T. Fig.1 shows such a plot for the three $YBCO/BZO$ samples along with $YBCO/YSZ$ for comparison. The virtue of plotting $\mid Z_s(T) \mid$ is that one can clearly see the lower $\lambda(0)$ in $YBCO/BZO$ which effectively translates to a higher superfluid density $(n_s/m) \sim 1/\lambda^2$.

In the superconducting state, the complex surface impedance is related to the complex conductivity and penetration depth: $Z_s(= R_s+iX_s) = \sqrt{i\mu_0\omega/(\sigma_1 - i\sigma_2)}$. Since the absolute values of R_s and X_s are known, it is possible to extract the complex conductivities:

$$\sigma_1 = \frac{2\mu_0\omega R_s X_s}{(2R_sX_s)^2 + (R_s^2 - X_s^2)^2}$$

$$\sigma_2 = \frac{\mu_0\omega(X_s^2 - R_s^2)}{(2R_sX_s)^2 + (R_s^2 - X_s^2)^2}$$

These quantities are important because they enable comparison with microscopic theories. The pair conductivity σ_2 is a representation of the superfluid density $\sigma_2 = (\mu_0\omega\lambda^2(T))^{-1}$ and is a convenient way of probing how the condensate builds up below the superconducting transition. The quasiparticle conductivity σ_1 is determined by the quasiparticle density as well as the quasiparticle scattering time.

In Fig.2, the temperature dependence of $\sigma_1(T)$ and $\sigma_2(T)$ are plotted for all the four samples, AE103, AE105, AE180 and AEXX. Two striking features emerge clearly from a comparison of the data:

(i) $\sigma_2(T)$ shows two distinct regions of variation above and below $\sim 60 - 70K$ in AE103, AE105 and AE180 samples in comparison with AEXX. Given the fact that $\lambda(0)$ is lower in $YBCO/BZO$ this implies enhanced pair conductivity in these samples.

(ii) The normal conductivity $\sigma_1(T)$ shows a new peak at around $80K(\sim 0.9T_c)$ in $YBCO/BZO$ crystals which is absent in $YBCO/YSZ$. This peak is greatly suppressed in AE105 as seen in Fig.2. We show later that there is a correlation between this peak and the normal state inelastic scattering rate of the samples. It is to be noted that the normal conductivity peak at $\sim 30 - 35K$ and a very sharp peak near T_c are present in all the samples.

Note that these two new features are both absent in all previously measured crystals. This is evident from the data on the $YBCO/YSZ$ sample shown in Fig.2. We emphasize that the $YBCO/YSZ$ data is indeed "canonical" of the samples prepared by previous growth methods. This is illustrated in Fig.3 which compares the $YBCO/YSZ$ data with that measured by us on an untwinned $LuBa_2Cu_3O_{6.95}$ sample [20] and by the UBC group on $YBa_2Cu_3O_{6.95}$ [27]. Note the excellent consistency of data on all previous samples with each other in Fig.3, and the systematic differences with the new data in Fig.2.

III. ANALYSIS AND DISCUSSION

A calculation of the high frequency conductivity requires proper incorporation of scattering effects along with self-consistent calculations of the gap and density of states. In addition anisotropy effects should also be included for the cuprate superconductors. While this has been done [21–23] for unconventional superconductors including those with a d-wave OP, these approaches are not easily amenable to comparison with experimental data.

Instead, in order to compare with the present experimental data we use a simpler "two-fluid" model of the form [24]:

$$\sigma(\omega, T) = \sigma_1 - i\sigma_2 = \frac{ne^2}{m}\left[\frac{f_n}{i\omega + 1/\tau(T)} - \frac{if_s}{\omega}\right]$$

where f_n and f_s represent the fractions of normal and superfluid (with $f_n + f_s = 1$), and τ is the relaxation time for normal electrons. In this model, the normal electrons have damping with the usual Drude conductivity at high frequencies, and the superconducting electrons have inertia but no damping. The quasiparticle and pair conductivities can be numerically calculated from:

$$f_s = (1 - f_n) = 1 - 2\left\langle\int_0^\infty \left(-\frac{\partial f}{\partial E}\right) d\epsilon\right\rangle$$

where $E = \sqrt{\epsilon^2 + \Delta^2(\phi, T)}$, and $\Delta(\phi, T)$ is the gap parameter, and $< .. >= \int_0^{2\pi} d\phi$ indicates an angular average over ϕ. The gap parameters are given by $\Delta(\phi, T) = \Delta_s(T)$ and $\Delta(\theta, T) = \Delta_d(T)\cos(2\phi)$ for s-wave and d-wave superconductors respectively. For $\Delta_s(T)$ and $\Delta_d(T)$ we use appropriate mean-field temperature dependences. The validity of this two-fluid approach, which is used frequently in s-wave superconductors following Mattis & Bardeen [25], has been discussed for d-wave superconductors by Hirschfeld, *et.al.* [22].

A. Comparison with models

We now discuss the comparison of the experimental data with detailed models which are implemented assuming various conditions for the gap parameters.

1. *Single d-wave order parameter: Its failure to describe the present results*

There is a general consensus that the superconducting order parameter symmetry in cuprates is not a simple s-wave type as is the case in conventional superconductors. A wealth of experimental results indicate unconventional pairing and more specifically point to the presence of nodes in the gap. A strong candidate which has been found to account for most of the properties in cuprates is the theory of d-wave superconductivity. A single complex d-wave order parameter has been proposed with a gap of the form: $\Delta(T) = \Delta_d(T)cos2\phi$ where ϕ specifies the orientation of the two-dimensional momentum of the Cooper pairs. This expression leads to two important signatures, namely, the order parameter goes to zero in certain k directions and also changes sign as one goes around the Fermi surface. Angle-resolved photoemission [26] and phase sensitive SQUID experiments [1] have shown strong evidence for this behavior. For experiments which measure quantities averaged over k-space (like the microwave penetration depth), the consequence of the d-wave gap will lead to features in the low temperature dependence which should be consistent with the presence of a finite density of states within the gap.

A linear low temperature dependence in YBCO single crystals first observed by UBC group [27] (and subsequently confirmed by others including ourselves in $YBCO$ [18,28] and also $Bi:2212$ [19]) has been claimed as prime evidence for nodes in the gap, which applies to d-wave symmetry among other possibilities. Rigorous calculations of the microwave conductivity in the framework of $d-$wave theories have also been done to explain the features observed in prior $YBCO/YSZ$ samples [22,23].

In Fig.3, a plot of $(\lambda^2(0)/\lambda^2(T))$ vs. reduced temperature $(t = T/T_c)$ for $YBCO/YSZ$ single crystals is shown. A comparison to detailed d-wave calculations has been carried out by us in an earlier publication [18]. Comparison shows that although the low temperature dependence is reproduced by calculations (not shown) using a weak coupling $d-$wave order parameter, the agreement is not very good at temperatures $T > 0.5T_c$, suggesting that strong coupling effects are needed.

For the $YBCO/BZO$ single crystals, the low temperature penetration depth $\lambda(T)$ is indeed linear for all 3 samples measured up to $\sim 20-25K$ with a characteristic slope $d\lambda/dT$ of about $4.5\mathring{A}/K$, similar to that of the $YBCO/YSZ$ samples. However deviation from linearity is observed above $25K$ for the $YBCO/BZO$ crystals due to the onset of the broad $60K$ bump. This is clearly evident from the plots of $\sigma_2(T)$ presented in Fig.2 which shows a non-monotonic dependence for AE103, AE180 and AE105 samples when compared to the AEXX curve. While a single order parameter may be reconciled at first glance for the $YBCO/YSZ$ data [18], it is impossible to do so for the results on the $BaZrO_3$ grown crystals [7]. Instead a two-component model has to be considered as is done below.

B. Comparison to decoupled two-component order parameters

The simplest way in which one can analyze a two-component system is to consider two parallel superconducting channels and to add their complex conductivities. The total conductivity can then be written as:

$$\sigma = \sigma_1 - i\sigma_2 = (\sigma_{1A} + \sigma_{1B}) - i(\sigma_{2A} + \sigma_{2B})$$

For ease of calculation we consider that the two components are decoupled with distinct transition temperatures, T_{cA} and $T_{cB}\,(> T_{cA})$. (We emphasize that in all likelihood the components are coupled, and furthermore there is only one phase transition at T_{cB}, with T_{cA} more of a crossover temperature, as discussed later). Calculations of the conductivities can be performed using the Mattis-Bardeen formalism introduced earlier. In an earlier paper, we had presented the qualitative model where for ease of calculation we used $s-$wave order parameters for both the A and B components [7]. In reality, it is essential to choose at least one component to be $d-$wave to produce the linear low temperature dependence. Using a combination of s and d gap symmetries, it is possible to obtain excellent quantitative fits to the observed experimental data for all the $YBCO/BZO$ single crystals.

Fig.4 shows the experimental data for σ_2 and σ_1 along with the fits obtained with the two component model assuming an (s+d) case for the A and B components. Good fits can also be obtained for (d+d) and (d+s) cases for the two components. The data for the AE103 sample only is presented in the figures for clarity. It is possible to obtain similar fits for the other $YBCO/BZO$ crystals and the fit parameters for all the samples are tabulated in Table II. A good agreement between the data and model is obvious. Best fits are obtained for the following *generic* choices:

1. A low temperature component A with $T_{cA} \sim 60K$ and a high temperature component B with $T_{cB} \sim 93K$.

2. A weak coupling $d-$ wave gap with $\Delta_B = 2.16k_BT_c$ for the the $B-$ component and an $s-$wave gap with $\Delta_A = 1.76k_BT_c$ or a weak-coupling $d-$ wave gap for the $A-$ component.

3. A lower fraction of $s-$wave (~ 0.3) than the $d-$wave part (~ 0.7).

4. Temperature dependent scattering rates $\tau_{A,B}^{-1} \equiv \Gamma_{A,B} = \Gamma_{A,B(0)}(e^{\alpha(t-1)} - e^{-\alpha}) + \Gamma^{*}_{A,B}$ were used for for σ_1. This exponential variation agrees with the suggestion that the scattering time increases rapidly below the transition temperature. The variation of τ_A and τ_B with temperature is plotted in bottom of Fig.4. *The detailed functional form is not as important as the key feature of rapid variation of τ_A below $65K$ and τ_B below $93K$.*

The two-component model also provides an explanation of the $YBCO/YSZ$ data as can be seen from Fig.5. The fit parameters (Table I) suggest that impurities suppress the order parameter for the A component(a smaller ratio 10% of the superfluid density n_{sA} as well as a weaker gap $\Delta_A(0)/k_BT_{cA} \sim 1.0$ are needed), as well as greatly enhancing the scattering rate τ_B^{-1} about 10 times larger for the B component. The rapid variation of τ_A below $50K$ is still needed to obtain the $30K$ peak in $\sigma_1(T)$ for the $YBCO/YSZ$ crystals.

The occurence of the low temperature normal conductivity peak in σ_1 at around $30K$, even though the superconducting transition temperatures are in excess of $90K$ in $YBCO$ crystals, has long been a puzzling feature. An exponential reduction of the quasiparticle scattering rate below T_c was invoked to account for this. However, the present data provides an explanation for the location of this peak, since in the present experimental results, it is natural to associate the two σ_1 peaks with the corresponding features in the pair condensate density as inferred from σ_2. Two types of pairing with different characteristic energy scales are clearly observed in these high quality $YBCO/BZO$ single crystals. In the $YBCO/YSZ$ samples, these energy scales are also present but their signatures are obscured by impurity scattering.

One aspect of the comparison should be noted. Because we have used a model in which the components are decoupled, the calculations necessarily show a sharp break at around $T_{cA} \sim 60K$, whereas the data display a smooth crossover. This is an indication that the decoupled model is too simplistic, and a coupled model is necessary. Indeed such calculations performed [66] within a Ginzburg-Landau framework lead to a smooth crossover in $\lambda^{-2}(T)$ in closer agreement with the experiments. However a full calculation of the conductivities requires a microscopic model which still needs to be implemented. (See also the remarks in the Summary section of this paper).

We note that there have been other discussions of multiple components (gaps or quasiparticles) in the cuprate superconductors. A two-gap model was proposed earlier by Klein et al. [29] to describe the data on $YBCO$ thin films with low cation disorder. In their case, however, low and high gaps both with $s-$wave symmetry and the same T_c were chosen to calculate the pair conductivity and the issue of σ_1 was not addressed in detail. Two-component behavior in 124 and underdoped 123 compounds have also been reported in Raman [30] and femtosecond optical response [31].

Anisotropic penetration depth measurements along the a and $b-$axes reported on untwinned $YBCO/YSZ$ single crystals [32]. Lower $\lambda(0)$ in the b-direction suggested superconductivity in the $Cu-O$ chains with the onset T_c same as that of the planes viz. $93K$. The similarity between $1/\lambda_a^2$ and $1/\lambda_b^2$ was taken as evidence that chain order parameter also has nodes in the gap. However, in our present data, additional superfluid response clearly turns on *below* $60K$ and if this is due to chains, then this would imply that chain superconductivity occurs at a lower temperature than the planes and would also directly contradict the conclusions reached in ref. [32]. Recent experiments on anisotropic thermal conductivity in detwinned $YBCO/YSZ$ single crystals have also revealed enhanced superfluid density below $\sim 55K$ which has been interpreted as due to chains [33]. This will be consistent with our observations of the microwave response in $YBCO/BZO$.

C. Near-Tc behavior:

We turn our attention now to the transition region close to T_c. The temperature dependence of the penetration depth $\lambda(T)$ is expected to reveal the characteristic nature of the superconducting gap as it opens up and also possible contributions due to fluctuations. In contrast to conventional superconductors, the low dimensionality and small coherence length in cuprates make them good candidates for studying the effect of superconducting fluctuations and in determining the universality class they belong to. While Ginzburg-Landau theory generally describes the region near the transition very well in conventional superconductors, it has been argued that in $YBCO$ assuming the simplest case of a *single* complex order parameter, it is possible to observe critical behavior which would give rise to fluctuations corresponding to the universality class of the three dimensional (3D) XY model. Transport and thermodynamic measurements in the presence of a magnetic field have been interpreted in terms of this model [34,35]. However, this has also been disputed by Roulin et al. [36] who argue that fits of the specific heat near T_c in YBCO single crystals for high magnetic fields do not weigh in favor of 3D XY scaling.

Penetration depth data close to the transition region will be influenced by the presence or absence of critical fluctuations. Specifically, a plot of $[\lambda(0)/\lambda(T)]^n$ as a function of T just below T_c is a useful indicator of the validity of standard mean-field or the 3D XY

models. While a mean-field behavior can be deduced if $[\lambda(0)/\lambda(T)]^2$ is linear in T, 3D XY would require $[\lambda(0)/\lambda(T)]^3$ to be linear in T. The latter behavior has been observed in penetration depth measurements by the UBC group [37] and has been interpreted as consistent with the critical behavior of the 3D XY model. It is important to note the the choice of the range of temperature over which one looks for effects due to fluctuations is crucial. The dynamical fluctuations in the frequency dependent microwave conductivity above T_c has been examined by Booth et al. [38]. They arrive at the conclusion that while the Gaussian fluctuations can account for the behavior over a larger range in temperature, just $1-2K$ above T_c, the behavior is dominated by critical fluctuations. It should be noted that the temperature dependence of $[\lambda(0)/\lambda(T)]^2$ from kinetic inductance measurements has shown mean-field dependence [39].

In a bid to investigate the transition region in our data on $YBCO/BZO$ and $YBCO/YSZ$ single crystals, we have plotted the penetration depth for all four crystals as a log-log plot against the reduced temperature $[(T_c-T)/T_c]$ shown in the top panel of Fig.6. It is clear that all the data show a linear behavior (with a negative slope) with typical values of the slope lying around 0.5. The appropriate $\lambda(0)$ and T_c values estimated from our R_s and X_s data for the three $YBCO/BZO$ samples (AE103, AE180, AE105) and the $YBCO/YSZ$ sample (AEXX) were taken to obtain the individual curves. Except the data for AE180 which has a slightly higher slope (~ 0.6), the other data form a set of parallel lines. This behavior is consistent with mean-field variation of the order parameter below T_c. To illustrate the point further, a plot of $[\lambda(0)/\lambda(T)]^2$ vs T is presented in the bottom panel of Fig.6 for one $YBCO/BZO$ crystal. The *linear* variation is quite obvious and is clearly different from the behavior reported for $YBCO$ single crystals in ref. [37]. The inset shows the same data plotted as $[\lambda(0)/\lambda(T)]^3$ vs T which is non-linear and rules out the possibility of 3D XY. The smooth variation of the $[\lambda(0)/\lambda(T)]^3$ vs T curve also indicates against the possibility of interpretation as a crossover behavior from 3D XY very near T_c to a mean-field like variation at lower temperatures. Our conclusion in this context would be that the near-T_c behavior in all $YBCO$ crystals is governed by standard mean-field expression. It is interesting to note that this universal behavior may also be indicative of a scenario against the possibility of a single order parameter. Absence of 3D XY correlations is not surprising if one considers unconventional pairing states with mixed symmetry.

D. Normal state scattering rate

Assuming a local $j-\hat{E}$ relation in the skin depth limit, the normal state surface resistance can be written as $R_n = \sqrt{\omega\mu_0\rho_n/2}$ where the microwave normal state resistivity is expected to be the same as the DC resistivity and $\rho_n = 2\Gamma\ \mu_0\lambda(0)^2$. Here $\lambda(0)$ is the London penetration depth and Γ is the normal state scattering rate. Taking $\rho_n = \rho_0 + \gamma T$ the resistivity values can be translated into the inelastic scattering rates given by $\Gamma\ = \gamma T/2\mu_0\lambda^2(0)$.

In Fig.7, we have plotted the normal state inelastic scattering rate as a function of temperature for $100K < T < 200K$ for all the $YBCO/BZO$ samples along with the data for $YBCO/YSZ$ crystal. Among the $YBCO/BZO$ single crystals, the Γ values as well as the slopes for AE103 and AE180 over the entire temperature range are lower than that for the AE105 sample. The $YBCO/YSZ$ AEXX sample has the largest Γ in this batch of crystals whose microwave surface impedance were measured in an identical manner. A comparison of this data with the $\sigma_1(T)$ data of Fig.2 shows a clear correlation between the normal state scattering rate and the new $80K$ quasiparticle conductivity peak. This peak is prominent only in AE180 and AE103 samples which have a lower scattering rate, is suppressed in AE105 which shows a larger Γ than the other two $YBCO/BZO$ samples and practically absent in AEXX which has the largest scattering rate. This remarkable correlation indicates the sensitive nature of the new conductivity peak to very small changes in impurity concentration and/or oxygen stoichiometry. Further studies in $YBCO/BZO$ crystals with transition-metal doping and variation of oxygen stoichiometry are needed to explore the correlation between the electronic properties in the normal state and the quasiparticle contribution in the superconducting state which is suggested by our present data.

IV. SUMMARY OF MICROWAVE PROPERTIES OF YBCO/BZO AND YBCO/YSZ CRYSTALS

We summarize below some of the microwave properties exhibited by the $YBCO/BZO$ crystals along with comparison of results on the previous class of $YBCO/YSZ$ samples. The key observations are:

1. The linear behavior of the low temperature penetration depth $\lambda(T) \propto T$ appears to be very robust and is observed in all samples with essentially the same slope. $\lambda(T)$ rises linearly with T upto $0.25T_c$ in $YBCO/BZO$ single crystals with a characteristic slope $(d\lambda/dT)$ of about $5\mathring{A}/K$. This linear variation is in agreement with the observations on $YBCO/YSZ$ crystals too and has been ascribed to the presence of nodes in the gap, and overall is considered a strong evidence for $d-$wave order parameter [27]. However, unlike the data in $YBCO/YSZ$, the full temperature dependence for $YBCO/BZO$ display a non-monotonic behavior which points to

the presence of an extra component in addition to a $d-$wave part.

A linear behavior of $\lambda(T)$ is also seen in good quality $BSCCO$ single crystals [19,60,61]. A T^2 behavior which has also been reported in $YBCO$ thin films [62], has been considered a consequence of inhomogeneties and additional scattering caused by impurities and disorder.

2. The surface resistance $R_s(T)$ of $YBCO/BZO$ shows a bump at around $30K$ as well as a broad bump at higher temperatures. In terms of conductivity, this results in two peaks occuring at $\sim 30K$ and $\sim 80K$. The ratio σ_1/σ_n of the peaks are much higher and cannot be explained due to coherence effects predicted by BCS theory. We have associated these two peaks with two different quasiparticle systems corresponding to components A and B as discussed earlier.

   In $YBCO/YSZ$, only the low temperature peak at $\sim 30K$ is seen. This was first observed at sub-THz [63] and at microwave frequencies [64]. To account for this feature, Bonn et al. [64] proposed an rapid increase in the inelastic scattering time (τ) below T_c followed by a reduction in carrier density at low temperatures.

3. The interpretation of the conductivity peak as arising from an interplay of increasing τ and decreasing n_{qp} as T is lowered has also been used here to account for the conductivity peak [63,64]. Such an interpretation necessarily requires a rapid variation of τ_B just below $93K$ and of τ_A below $65K$ as is evident from Fig. 4 in $YBCO/BZO$.

   It is to be noted that in $BSCCO$, our results [19] do not show any conductivity peak in σ_1 below T_c but rather σ_1/σ_n rises monotonically as T is lowered. However another study [60]claims to see a small reduction in σ_1/σ_n at very low temperatures suggestive of a conductivity peak.

4. It is important to note that *the two temperature scales of* $93K$ *and* $65K$ *are present in* $YBCO/YSZ$ *also.* This can be seen from the fact that two component analysis also describes the $YBCO/YSZ$ data, as shown in Fig.5, provided a suppressed n_{sA} and τ_B are used. This suggests that in the $YBCO/YSZ$ crystals, impurities lead to suppression of the pairing density of the A component, as well as greatly enhanced scattering of the B component.

5. A very sharp peak in σ_1 just below T_c at around $91 - 92K$ is seen in all ($YBCO/BZO$ as well as $YBCO/YSZ$) samples, so that there are a total of 3 conductivity peaks. This peak near T_c has been ascribed to fluctuations [40] or inhomogeneities [65]. In the $YBCO/BZO$ samples this peak is extremely sharp and further attests to the high sample quality.

6. The temperature scale of $65K$ naturally raises the possibility of a multi-phase sample with regions of $YBCO_{6.5}$. We have considered this issue very carefully and several experiments show that this is *conclusively* ruled out. In-situ resisitivity meaasurements at high temperatures have shown that the crystals can be reversibly oxygenated-deoxygenated, and that the diffusion constants are well characterized, indicating nothing unusual about the oxygenation of these samples [8]. Note also that the $YBCO/YSZ$ sample $AEXX$ was oxygenated using the same procedures but did not display the new features in the conductivity. Furthermore, the similarity of the AE180 data with the other samples conclusively shows that even local O vacancies are not responsible for the present results. This is because in AE180, high pressure oxygenation breaks up O deficient clusters, as evidence by the elimination of the fishtail anomaly in samples prepared by this method.

7. Our measurements on both $YBCO/BZO$ and $YBCO/YSZ$ single crystals are consistent with mean-field behavior rather than $3DXY$ close to T_c. Near-T_c variation of $1/\lambda^2$ has been analysed in terms of $3DXY$ scaling by Kamal et al. [37] in their $YBCO/YSZ$ crystals. While a more rigorous study of the fluctuation contributions below and above T_c by Booth et al. [38] indicated that $3DXY$ scaling is seen only over a limited temperature range, kinetic inductance measurements by Lemberger et al. [39] on thin films suggest mean-field behavior, in agreement with the conclusions of this paper.

8. It should be noted that the pairing onset below $65K$ in the $\sigma_2(T)$ is quite broad, and indicates that this is not likely to be a critical point. *Thus we believe that there is only one transition at* $T_c = 93.4K$, *with a crossover at* $65K$ *where the additional pairing channel opens up.* Furthermore, although we have used a decoupled scenario to analyze the data, it is very likely that the OP's are coupled. This is confirmed by calculations of the superfluid density using a simple Ginzburg-Landau free energy for two coupled OP, which reproduce the main features of the $\lambda^{-2}(T)$ data [66]. At high temperatures $T_c > T > T_{cA}$, the symmetry is predominantly of type B, although a small $A-$component is also induced due to the coupling. At lower temperatures $T < T_{cA}$, the $A-$component grows so

that both components (and hence a mixed symmetry) are present. Microscopic calcuations of thermodynamic properties of superconducting lattice fermions which also have multiple pairing channels also show that the thermodynamic signatures, such as specific heat cusps, are weaker in the subdominant channels which appear at lower temperatures than in the main channel [44].

While we have presented a simple phenomenological two-component model in this paper to account for the two conductivity peaks in $YBCO/BZO$, microscopic calculations (similar to those based on a single $d-$wave order parameter [21–23]) need to be done for the surface impedance of a two-component superconductor. Furthermore, the analysis used here assumes phase coherence throughout the sample and does not include contributions arising from phase fluctuations [67,68].

V. RELATION TO MICROSCOPIC THEORIES

Models based on any type of mixed order parameter symmetry would yield results consistent with our experimental observations in the $YBCO/BZO$ system. Mixed order parameter symmetry and multi-component behavior of the order parameter has been addressed in several theoretical papers which can be broadly classified along the following categories:

(1) $s + d, s + id$: It has been argued that the orthorhombic structure of $YBCO$ naturally leads to a mixing of s and d order parameter components [3]. Several theories [2,41–45] advocate to this general concept of a mixed $s + d$ OP and have successfully developed models which can describe the experimental results in $YBCO$. This appears to be consistent with photoemission data on overdoped $BSCCO$ also [46,41]. Phenomenological [41] and microscopic theories [47] have been considered. The work of ref. [47] indicates that the system likely goes from a $d-$wave state at high temperatures to an $s + id$ state at low T.

(2)*Chain-Plane coupling:* The presence of $Cu - O$ chains in addition to planes raises the possibility of different superconducting condensates with different pairing energies residing on chains and planes. This can effectively lead to a two-component system exhibiting two different gaps [48]. Coupling between chain and plane bands has been proposed [49] to account for both the s and d characteristics displayed by $YBCO$.

(3)*Multi band models and Fermi pockets:* Theoretical treatments based on multi band models have been presented which considers the interband interactions [50,49,51–53]. This general framework also reproduces the essential features of a two-component superconductor. The nature of the Fermi surface could be important in determining the possibility of multiple pairing energies. The presence of pockets with d and $g-$ wave symmetries has been recently discussed [54].

(4) *Surface states and Time Reversal Symmetry breaking:* The possibility of mixed order parameter symmetry at the surface leading to breaking time reversal symmetry has been suggested [55,56]. Recent observation of Andreev bound states at the surface of $YBCO$ [57,58] strongly suggests this possibility.

(5) *Interlayer Tunneling:* In a recent paper, Xiang and Wheatley [59] presented a model based on proximity effect incorporating a microscopic pair tunneling process which couples the $Cu - O$ chains and planes in $YBCO$, to account for the experimental results on $YBCO/YSZ$ data from the UBC group [32]. Our present results on the $YBCO/BZO$ crystals suggests that within the interlayer tunneling model, single electron tunneling processes could account for the features observed in our data.

VI. CONCLUSION

In summary, we have shown that high quality single crystals of $YBCO$ grown in $BaZrO_3$ crucibles exhibit features in their microwave properties, which are inconsistent with a pure d-wave OP and instead point to the occurence of multi-component superconductivity.The measurements reveal the presence of two pairing temperatures corresponding to two superconducting (pair/quasiparticle) components in the optimally doped compound. This should be borne in mind and careful studies should be performed on high quality materials to further explore these issues.

ACKNOWLEDGMENTS

Work at Northeastern was supported by NSF-DMR-9623720, and at Geneva by the Fonds National Suisse de la Recherche Scientifique. We thank R. S. Markiewicz, Balam A. Willemsen and D. P. Choudhury for useful discussions.

---

[1] *See* D. J. Van Harlingen, *Rev. Mod. Phys.* **67**, 515 (1995) *and references therein.*

[2] K. A. Muller, *Nature* **377**, 133 (1995).

[3] B. E. C. Koltenbah and R. Joynt, *Rep. Prog. Phys.* **60**, 23 (1997).

[4] A. Erb, E. Walker and R. Flükiger, *Physica C* **245**, 245 (1995).

[5] H. Casalta, P. Schleger, P. Harris, B. Lebech, N. H. Andersen, R. Liang, P. Dosanjh and W. N. Hardy, *Physica C* **258,** 321 (1996).

[6] H. Ikuta and D. M. Ginsberg, *J. Supercond.* **9,** 259 (1996).

[7] H. Srikanth, B. A. Willemsen, T. Jacobs, S. Sridhar, A. Erb, E. Walker and R. Flükiger, *Phys. Rev. B* **55**, **R**14733 (1997).

[8] A. Erb, B. Greb and G. Müller-Vogt, *Physica C* **259**, 83 (1996).

[9] B. G. Storey, M. A. Kirk and L. D. Marks, *Physica C* **246**, 46 (1995).

[10] E. Brecht,W. W. Schmahl, M. Rodewald, G. Miehe, H. Fuess, N. H. Andersen, J. Hanssmann and Th. Wolf, *Physica C* **265**, 53 (1996).

[11] I. Maggio-Aprile, Ch. Renner, A. Erb, E. Walker and Ø. Fischer, *Phys. Rev. Lett.* **75**, 2754 (1995).

[12] A. Erb, J.-Y. Genoud, F. Marti, M. Däumling, E. Walker and R. Flükiger, *J. Low Temp. Phys.* **105** 1023 (1996).

[13] J.-Y. Genoud, B. Revaz, A. Erb, A. Mirmelstein, G. Triscone and A. Junod in *Proc. LT21 Conference, Prague, Czech Republic, Aug. 1996*, to be published in Czech J. Phys. Supplement.

[14] A. Junod, M. Roulin, J.-Y. Genoud, B. Revaz, A. Erb and E. Walker, *Physica C* **275**, 245 (1997); M. Roulin, A. Junod, A. Erb and E. Walker, *J. Low Temp. Phys.* **105**, 1099 (1996).

[15] I. Maggio-Aprile, Ch. Renner, A. Erb, E. Walker and O. Fischer, *J. Low Temp. Phys.* **105**, 1129 (1996).

[16] M. V. Indenbom, C. J. van der Beek, V. Berseth, W. Benoit, G. D'Anna, A. Erb, E. Walker, R. Flükiger, *Nature* **385**, 702 (1997).

[17] S. Sridhar and W. L. Kennedy, *Rev. Sci. Instrum.* **59**, 531 (1988).

[18] T. Jacobs, S. Sridhar, C. T. Rieck, K. Scharnberg, T. Wolf and J. Halbritter, *J. Phys. Chem. Solids* **56**, 1945 (1995).

[19] T. Jacobs, S. Sridhar, Qiang Li, G. D. Gu and N. Koshizuka, *Phys. Rev. Lett.* **75**, 4516 (1995).

[20] J.Buan, C.C.Huang, A.M.Goldman, Oriol T.Valls, T.Jacobs, Nathan Israeloff, S.Sridhar, C.R.Shih, Branko P.Stojkovic, J.-Z.Liu, Robert Shelton, and H.D.Yang, *Phys. Rev. B.*, **45**, 7462 (1996).

[21] R. A. Klemm, K. Scharnberg, D. Walker and C. T. Rieck, *Z. Phys. B* **72**, 139 (1988).

[22] P. J. Hirschfeld, W. O. Puttika and D. J. Scalapino, *Phys. Rev. B* **50**, 10250 (1994).

[23] S. Hensen, G. Müller, C. T. Rieck and K. Scharnberg, *preprint* (1997).

[24] J. R. Waldram, *Superconductivity of Metals and Cuprates* (IOP, Bristol, 1996).

[25] D. C. Mattis and J. Bardeen, *Phys. Rev.* **111**, 412 (1958).

[26] Z. -X. Shen, D. S. Dessau, B. O. Wells, D. M. King, W. E. Spicer, A. J. Arko, D. Marshall, L. W. Lombardo, A. Kapitulnik, P. Dickinson, S. Doniach, J. diCarlo, A. G. Loeser and C. H. Park, *Phys. Rev. Lett.* 70*,* 1553 (1993).

[27] W. N. Hardy, D. A. Bonn, D. C. Morgan, R. Liang and K. Zhang, *Phys. Rev. Lett.* **70**, 3999 (1993).

[28] J. Mao, D. H. Wu, J. L. Peng, R. L. Greene and S. M. Anlage, *Phys. Rev. B* **51,** 3316 (1995).

[29] N. Klein, N. Tellman, H. Schulz, K. Urban, S. A. Wolf and V. Z. Kresin, *Phys. Rev. Lett.* 71*,* 3355 (1993).

[30] E. T. Heyen, M. Cardona, J. Karpinski, E. Kaldis and S. Rusiecki, *Phys. Rev. B* **43**, 12958 (1991).

[31] C. J. Stevens, D. Smith, C. Chen, J. F. Ryan, B. Pobodnik, D. Mihailovic, G. A. Wagner and J. E. Evetts *Phys. Rev. Lett.* **78**, 2212 (1997).

[32] K. Zhang, D. A. Bonn, R. Liang and W. N. Hardy, *Phys. Rev. Lett.* **73***,* 2484 (1994).

[33] R. Gagnon, S. Pu, B. Ellman and L. Taillefer, *Phys. Rev. Lett.* 78*,* 1976 (1997).

[34] M. B. Salamon, J. Shi, N. Overend and M. A. Howson, *Phys. Rev. B* **47**, 5520 (1993).

[35] N. Overend, M. A. Howson and I. D. Lawrie, *Phys. Rev. Lett.* 72*,* 3238 (1994).

[36] M. Roulin, A. Junod and J. Muller, *Phys. Rev. Lett.* 75*,* 1869 (1995).

[37] S. Kamal, D. A. Bonn, N. Goldenfeld, P. J. Hirschfeld, R. Liang and W N. Hardy, *Phys. Rev. Lett.* **73***,* 1845 (1994).

[38] J. C. Booth, D. H. Wu, S. B. Qadri, E. F. Skelton, M. S. Osofsky, A. Piqué and S. M. Anlage, *Phys. Rev. Lett.* **77***,* 4438 (1996).

[39] T. R. Lemberger, E. R. Ulm, K. M. Paget and V. C. Matijasevic, *SPIE Proceedings* **2696,** 211 (1996).

[40] M. L. Horbach, W. van Sarloos and D. A. Huse, Phys. Rev. Lett. **67**, 3464 (1991)

[41] J. Betouras and R. Joynt, *Europhys. Lett.***1**, 119 (1995).

[42] C. O'Donovan and J. P. Carbotte, *Phys. Rev. B* **52**, 16208 (1995).

[43] M. T. Beal-Monod and K. Maki, *Phys. Rev. B* **53**, 5775 (1996).

[44] E. Otnes and A. Sudbo, (preprint) (1997).

[45] D. van der Marel, *Phys. Rev. B* **51,** 1147 (1995).

[46] J. Ma, C. Quitmann, R. J. Kelley, H. Berger, G. Margaritondo and M. Onellion, *Science* **267**, 862 (1995).

[47] Y. Ren, W. Xu and C. S. Ting, *Phys. Rev. B* **53,** 2249 (1996).

[48] V. Z. Kresin and S. A. Wolf, *Phys. Rev. B* **46**, 6458 (1992).

[49] R. Combescot and X. Leyronas, *Phys. Rev. Lett.* 75*,* 3732 (1995).

[50] P. H. Dickinson and S. Doniach, *Phys. Rev. B* **47**, 11447 (1993).

[51] R. Combescot, *cond-mat preprint* 9707241 (1997).

[52] A. A. Golubov, M. R. Trunin, A. A. Zhukov, O. V. Dolgov and S. V. Shulga, *J. Phys. I France* **6**, 2275 (1996).

[53] P. K. Mohanty and A. Taraphder, *cond-mat preprint* 9703180 (1997).

[54] P. V. Shevchenko and O. P. Sushkov *preprint* 1997.

[55] R. B. Laughlin, *Physica C* **234**, 280 (1994).

[56] A. M. Tikofsky and D. B. Bailey, *Phys. Rev. B* **52**, 9194 (1995).

[57] M. Covington, M. Aprili, E. Paraoanu, L. H. Greene F. Xu, J. Zhu, and C. A. Mirkin, *Phys. Rev. Lett.* **79**, 277 (1997).

[58] M. Fogelstrom, D. Rainer, J. A. Sauls, *Phys. Rev. Lett.* **79**, 281 (1997).

[59] T. Xiang and J. M. Wheatley, *Phys. Rev. Lett.* 76*,* 134 (1996).

[60] S-F. Lee, D. C. Morgan, R. J. Ormeno, D. M. Broun, R. A. Doyle and J. R. Waldram, *Phys. Rev. Lett.* **77,** 735 (1996).

[61] T.Shibauchi, N. Katase, T. Tamegai and K. Uchinokura, *Physica C* **254,** 227 (1996).

[62] Z. Ma, R. C. Taber, L. W. Lombardo, A. Kapitulnik, M. R. Beasley, P. Merchant, C. B. Eom, S. Y. Hou and J. M. Phillips, *Phys. Rev. Lett.* **71**, 781 (1993).

[63] M. C. Nuss, P. M. Mankiewich, M. L. O'Malley, E. H. Westerwick and P.B. Littlewood, *Phys. Rev. Lett.* **66**, 3305 (1991).

[64] D. A. Bonn, P. Donsajh, R. Liang and W. N. Hardy, *Phys. Rev. Lett.* 68*,* 2390 (1992).

[65] H. K. Olsson and R. H. Koch, Phys. Rev. Lett. **68**, 2406 (1992)

[66] S. Sridhar (*unpublished*).

[67] V. J. Emery and S. A. Kivelson, *Nature* **374,** 434 (1995).

[68] E. Roddick and D. Stroud, *Phys. Rev. Lett.* **74,** 1430 (1995).

YBCO/YSZ	**YBCO/BZO**
Crucible: Yttria-stabilized Zirconia (YSZ)	Crucible: $BaZrO_3$
Crystal Purity: 99.5 to 99.95 % [5]	Crystal Purity: 99.995 % [8]
$T_c = 93.2$ to $93.5K$	$T_c = 93.2$ to $93.5K$
Estimated $\lambda(0) \sim 1600 - 2000\mathring{A}$	Estimated $\lambda(0) \sim 1000 - 1400\mathring{A}$
Flux lattice not imaged with STM	Flux lattice imaged with cryogenic STM [11]
Schottky anomaly present in specific heat	Schottky anomaly suppressed in high pressure oxygenated $O_{6.95}$ and eliminated in O_7 [14]
Large "Fishtail effect" in Magnetization	"Fishtail" greatly suppressed in high pressure oxygenated $O_{6.95}$ and eliminated in O_7 [12]
Substantial Pinning due to impurities	Very low pinning evidenced by extremely low critical currents and observation of flux lattice melting [16]

TABLE I. A comparison of some material and physical properties of $YBCO/BZO$ and $YBCO/YSZ$ single crystals.

Samples	**AE103** (*d* + *d*)	**AE105** (*d* + *d*)	**AE180** (*d* + *d*)
Components	**A(0.6), B(0.4)**	**A(0.6), B(0.4)**	**A(0.48), B(0.52)**
$T_{c(A,B)}$	63K, 93K	59K, 93K	58K, 93K
$\Gamma_{(A,B)(0)}$ meV	11, 8	10, 13	7, 13
α	12, 25	10, 8	9, 14
$\Gamma^*_{(A,B)}$ meV	0.08, 0.6	0.08, 1.1	0.06, 1.2

Samples	**AE103** (*s* + *d*)	**AE105** (*s* + *d*)	**AE180** (*s* + *d*)
Components	**A(0.6), B(0.4)**	**A(0.6), B(0.4)**	**A(0.45), B(0.55)**
$T_{c(A,B)}$	63K, 93K	59K, 93K	58K, 93K
$\Gamma_{(A,B)(0)}$ meV	12, 8	18, 14	10, 16
α	11, 25	11, 6	10, 16
$\Gamma^*_{(A,B)}$ meV	0.05, 0.8	0.04, 0.4	0.02, 1.4

Samples	**AE103** (*d* + *s*)	**AE105** (*d* + *s*)	**AE180** (*d* + *s*)
Components	**A(0.78), B(0.22)**	**A(0.78), B(0.22)**	**A(0.68), B(0.32)**
$T_{c(A,B)}$	63K, 93K	59K, 93K	58K, 93K
$\Gamma_{(A,B)(0)}$ meV	20, 7	12, 9	10, 10
α	11, 21	11, 10	9, 14
$\Gamma^*_{(A,B)}$ meV	0.24, 0.52	0.06, 0.01	0.1, 0.4

TABLE II. Fit parameters for the three $YBCO/BZO$ crystals using the several two-component scenarios. For the $YBCO/YSZ$ case, fits shown in Fig. 5 using the two-component model are generated using the following parameters: Components: A(0.1) and B(0.9); $T_cA, B = 60, 92K$; $\Gamma_{(A,B)(0)} = 10, 14$; $\alpha = 7, 12$; $\Gamma^*_{(A,B)} = 0.1, 0.01$. While the numbers are identical for (s + d) and (d + d) cases, (d + s) does not fit the data.

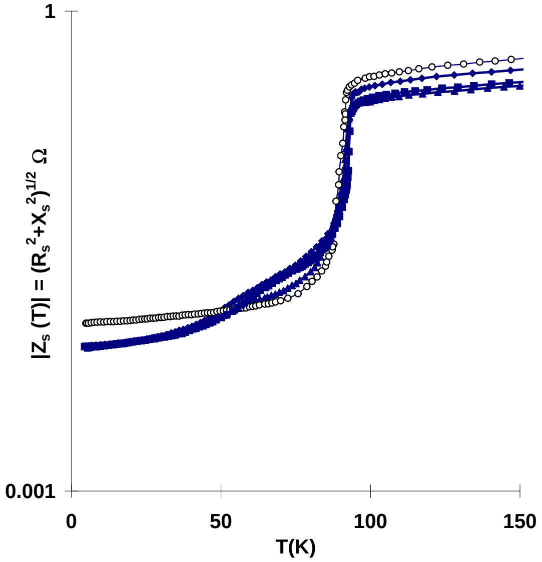

FIG. 1. Magnitude of surface impedance amplitude $\mid Z_s(T) \mid$ of $YBCO/BZO$ and $YBCO/YSZ$ single crystals. Filled symbols are used for BZO grown crystals: AE103 (filled squares), AE180 (filled triangles) and AE105 (filled diamonds). The data for YSZ grown AEXX (open circles) is also shown. The plot emphasizes the fact that $\lambda(0)$ for all the $YBCO/BZO$ crystals is lower than that of $YBCO/YSZ$.

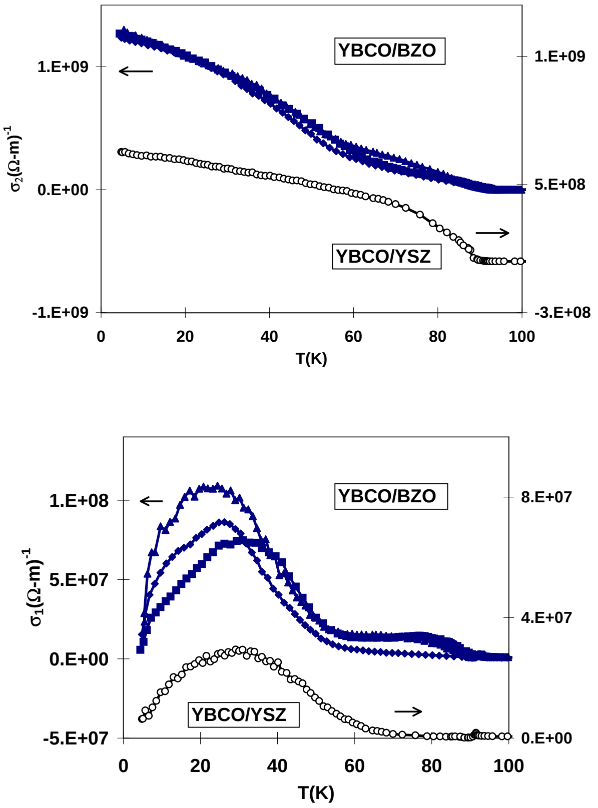

FIG. 2. Complex conductivities σ_2 (top panel) and σ_1 (bottom panel). The $YBCO/BZO$ data are shown in filled symbols and the $YBCO/YSZ$ data in open circles. Note the extra pairing at around $60K$ in σ_2 and the new peak at $80K$ in σ_1 in $YBCO/BZO$, both absent in $YBCO/YSZ$ data.

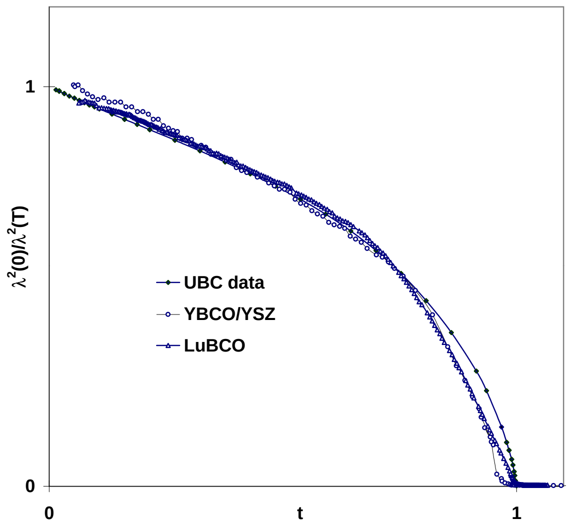

FIG. 3. Superfluid density of the YBCO/YSZ single crystal (AEXX) plotted against reduced temperature. Data for an untwinned YSZ grown $LuBCO$ crystal and the UBC data are also shown for comparison.

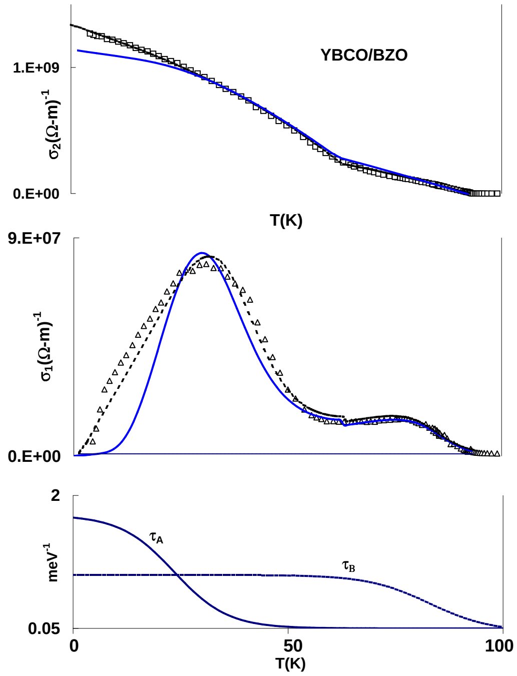

FIG. 4. σ_2 and σ_1 data for $YBCO/BZO$ single crystal (AE103) along with the fits generated using a decoupled two-component model (s + d) [solid line] and (d + d) (dashed line), discussed in the text. The bottom panel shows the variation of scattering times τ_A and τ_B below the T_c for A and B components for the (s+d) case. Essentially similar fits can be obtained for (d + s) case (not shown).

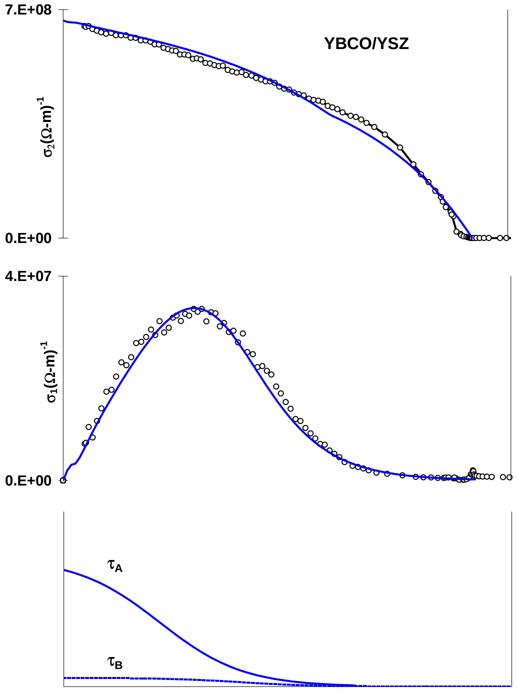

FIG. 5. σ_2 and σ_1 data for $YBCO/YSZ$ single crystal (AEXX) along with the fits generated using a decoupled two-component model (s + d) discussed in the text. The bottom panel shows the variation of scattering times τ_A and τ_B below the T_c for A and B components for the (s+d) case. The fit is identical with similar parameters for the (d + d) case. The (d + s) case does not fit the data.

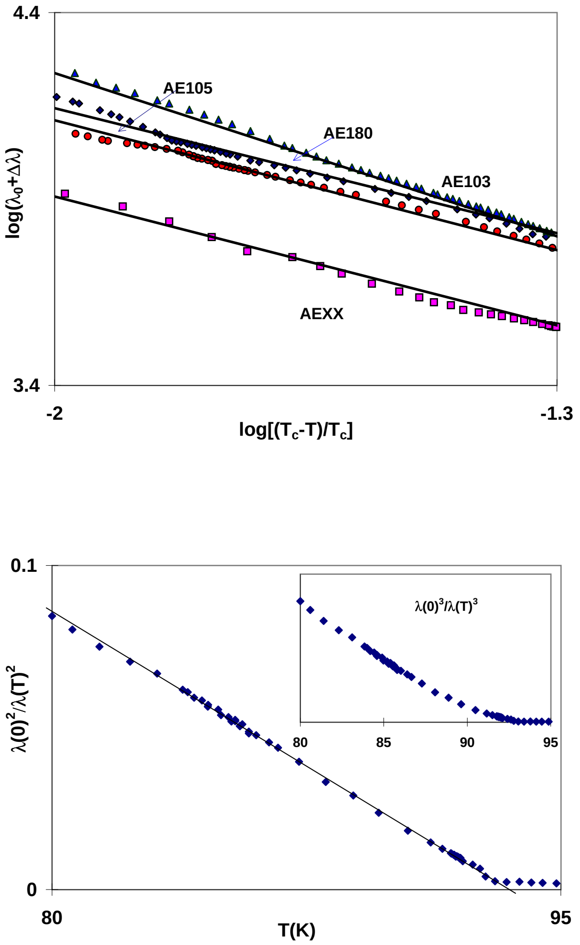

FIG. 6. Top panel: Penetration depth near T_c shown in a log-log scale. The data sets indicate a similar variation in all four samples, with a slope of 0.5 indicating mean field behavior. Bottom panel: Plot of the superfluid density, $[\lambda(0)/\lambda(T)]^2$ vs T just below T_c for AE103 crystal. The solid line is a guide to the eye indicating the linear variation consistent with mean-field behavior. Inset shows $[\lambda(0)/\lambda(T)]^3$ vs T for the same data in which the curvature is clearly evident indicating disagreement with the 3D XY model.

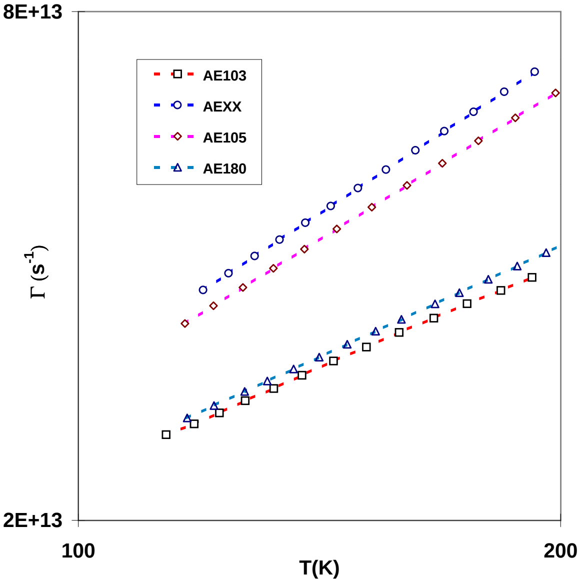

FIG. 7. The normal state inelastic scattering rate for all four samples. The data for AE103 and AE180 have lower values and smaller slope in comparison to AEXX and AE105 samples.